Title: Expression of ecto-nucleoside triphosphate diphosphohydrolase3 (NTPDase3) in the female rat brain during postnatal development

Author: Ivana Grković Ivana Bjelobaba Nataša Mitrović Irena Lavrnja Dunja Drakulić Jelena Martinović Miloš Stanojlović Anica Horvat Nadežda Nedeljković

PII: S0891-0618(15)30042-9
DOI: http://dx.doi.org/doi:10.1016/j.jchemneu.2016.04.001
Reference: CHENEU 1396

To appear in:

Received date: 16-11-2015
Revised date: 16-3-2016
Accepted date: 1-4-2016

Please cite this article as: Grković, Ivana, Bjelobaba, Ivana, Mitrović, Nataša, Lavrnja, Irena, Drakulić, Dunja, Martinović, Jelena, Stanojlović, Miloš, Horvat, Anica, Nedeljković, Nadežda, Expression of ecto-nucleoside triphosphate diphosphohydrolase3 (NTPDase3) in the female rat brain during postnatal development.Journal of Chemical Neuroanatomy http://dx.doi.org/10.1016/j.jchemneu.2016.04.001

Expression of ecto-nucleoside triphosphate diphosphohydrolase3 (NTPDase3) in the female rat brain during postnatal development

Ivana Grković[a], Ivana Bjelobaba[b], Nataša Mitrović[a], Irena Lavrnja[b], Dunja Drakulić[a], Jelena Martinović[a], Miloš Stanojlović[a], Anica Horvat[a], Nadežda Nedeljković[c]

[a] Department of Molecular Biology and Endocrinology, VINČA Institute of Nuclear Sciences, University of Belgrade, Belgrade, Serbia

[b] Institute for Biological Research "Siniša Stanković," University of Belgrade, Belgrade, Serbia

[c] Institute for Physiology and Biochemistry, Faculty of Biology, University of Belgrade, Belgrade, Serbia

*Corresponding author (current address):
Ivana Grković, PhD
Department of Molecular Biology and Endocrinology
VINČA Institute of Nuclear Sciences
University of Belgrade
Mike Petrovića Alasa 12-14
11001 Belgrade
Serbia
e-mail: istanojevic@vinca.rs

Highlights

- NTPDase3 is the membrane-bound ecto-enzyme which hydrolyzes extracellular ATP
- Developmental expression of NTPDase3 was analyzed in female rat brain at several postnatal ages (PD7–PD90)
- Faint NTPDase3-imunoreactivity (*ir*) was observed at PD7 and gradually increased in PD15 and PD20 at clusters of hypothalamic neurons.
- NTPDase3-*ir* fibers were first observed at PD20.
- NTPDase3- *ir* fiber density and the varicose appearance increased until the adulthood.

Abstract

Nucleoside triphosphate diphosphohydrolase3 (NTPDase3) is membrane-bound ecto-enzyme which hydrolyzes extracellular ATP, thus modulating the function of purinergic receptors and the pattern of purinergic signaling. Here we analyzed the developmental expression of NTPDase3 in female hypothalamus, cerebral cortex and hippocampal formation at different postnatal ages (PD7–PD90) by qRT-PCR and immunohistochemistry. In hypothalamus and hippocampus, a similar developmental profile was seen: NTPDase3 gene expression was stable during postnatal development and increased in adults. In the cortex, upregulation of NTPDase3 mRNA expression was seen at PD15 and further increase was evidenced in adults. Immunohistochemical analysis at PD7 revealed faint neuronal NTPDase3 localization, in dorsal hypothalamus. The immunoreactivity (*ir)* gradually increased in PD15 and PD20, in clusters of cells in the lateral, ventral and dorsomedial hypothalamus. Furthermore, in PD20 animals, NTPDase3-*ir* was detected on short fibers in the posterior hypothalamic area, while in PD30 the fibers appeared progressively longer and markedly varicose. In adults, the strongest NTPDase3-*ir* was observed in collections of cells in dorsomedial hypothalamic nucleus, dorsal and lateral hypothalamus and in several thalamic areas, whereas the varicose fibers traversed entire diencephalon, particularly paraventricular thalamic nucleus, ventromedial and dorsomedial hypothalamic nuclei, the arcuate nucleus and the prefornical part of the lateral hypothalamus. The presumably ascending NTPDase3-*ir* fibers were first observed in PD20; their density and the varicose appearance increased until the adulthood. Prominent enhancement of NTPDase3-*ir* in the hypothalamus coincides with age when animals acquire diurnal rhythms of sleeping and feeding, supporting the hypothesis that this enzyme may be involved in regulation of homeostatic functions.

Key words: Ecto-nucleoside triphosphate diphosphohydrolase (NTPDase3); postnatal development; hypothalamus; varicose fibers; feeding/sleeping behavior.

Abbreviations

ATP, adenosine triphosphate; ADP, adenosine diphosphate; Arch, arcuate nucleus; *chp*, choroid plexus; CM, central medial thalamic nucleus; D3V, third ventricle; DMC, compact part of dorsomedial hypothalamic nucleus; DMD, dorsomedial hypothalamic nucleus; DMV, ventral part of dorsomedial hypothalamic nucleus; Hip, hippocampus; IMD, intermmediodorsal thalamic nucleus; LH, lateral hypothalamus; LSI, lateral septal nucleus; M2, secondary motor area; MHb, medial habenular nucleus; MoDG, molecular layer of dentate gyrus; PH, posterior hypothalamic nucleus; PHD, posterior hypothalamic area; Pir, piriform cortex; PVP, paraventricular thalamic nucleus; Rh, rhomboid thalamic nucleus; VMH, ventromedial hypothalamic nucleus; VPM, ventral posteromedial thalamic nucleus; S2, secondary somatosensory cortex; slm, stratum lacunosum moleculare

1. Introduction

Extracellular adenosine triphosphate (ATP) acts as gliotransmitter, neurotransmitter, neuromodulator and trophic factor, controlling excitability, transmission and synaptic plasticity (Cunha and Ribeiro, 2000; Rodrigues *et al.*, 2005) during both embryonic and postnatal development of the central nervous system (CNS) (Dias *et al.*, 2013; Wieraszko, 1996; Zimmermann, 2006). By acting at two distinct classes of P2 receptors, ligand-gated P2X1-7 and G-protein coupled P2Y1-13 (Burnstock, 2007), extracellular ATP induces myriad of cellular actions in the CNS (for review, see Burnstock 2007, Zimmermann et al. 2012). The effects induced by ATP are under control of ectonucleotidase enzyme family, which catalyze sequential hydrolysis of extracellular ATP to ADP, AMP and adenosine (Zimmermann *et al.*, 2012).

In the rat brain, the ectonucleotidase family includes ecto-nucleoside triphosphate diphosphohydrolases1-3 (NTPDase1-3), which hydrolyze ATP and ADP to AMP, and ecto-5′-nucleotidase (eN), which catalyzes the final step of the conversion of AMP to adenosine. Individual members of NTPDase family differ in several respects, including their substrate preferences. Specifically, NTPDase1 uses ATP and ADP equally well to produce AMP, while NTPDase2 preferentially dephosphorylates ATP to ADP. NTPDase3 is the functional intermediate between the previous two, as it hydrolyzes both ATP and ADP with molecular ratio of about 1:0.3 (Smith and Kirley, 1998), leading to transient accumulation of ADP (Kukulski *et al.*, 2005). Therefore, NTPDase2 and NTPDase3 produce agonists which act at ADP-sensitive purinoceptors, such as P2Y1, P2Y12 and P2Y13 (Abbracchio *et al.*, 2006).

Members of ectonucleotidase family have a wide distribution in the brain, although individual members exhibit marked regional and cell-type specific localization (Bjelobaba *et al.*, 2007; Braun *et al.*, 2000; Langer *et al.*, 2008; Wang and Guidotti, 1998; Wink *et al.*, 2006). Among NTPDases expressed in the brain, the most restricted and exclusively neuronal

localization is observed for NTPDase3. Somatic NTPDase3 localization was observed only in the midline regions of the brain: in the thalamus and hypothalamus, the medulla oblongata (Belcher *et al.*, 2006) and in the spinal cord (Vongtau *et al.*, 2011). NTPDase3-expressing neuronal fibers are abundantly present in the midline regions of the brain, while scattered NTPDase3 positive axon-like processes with prominent varicosities were also observed in the cerebral cortex, hippocampus and basal ganglia (Belcher *et al.*, 2006; Bjelobaba *et al.*, 2010). It should be noted that nearly all of the NTPDase3-immunoreactive (*ir*) hypothalamic neurons and the vast majority of NTPDase3-*ir* fibers express hypocretin-1/orexin-A, suggesting its role in the autonomic and hormone-regulated behaviors, such as food intake, sleep-wake cycle, and reproduction (Belcher *et al.*, 2006). The involvement of the enzyme in the reproductive behaviors is further substantiated with the finding that in females, the expression of NTPDase3 in the sex-related regions of the medial and lateral hypothalamus can be modulated by exogenously administrated 17β-estradiol (Kiss *et al.*, 2009). Considering that the hypothalamus, cerebral cortex and hippocampus are highly estrogen responsive brain regions, the present study has been designed to investigate the developmental profile of NTPDase3 expression in the female rat brain. We also wanted to test if ovariectomy influences the expression levels of NTPDase3 in the selected brain regions of an adult female rats. Because regional and local distribution of individual NTPDases crucially affects the type and extent of P2 receptor signaling, essential for normal brain functioning, it is important to determine whether the NTPDase3 contributes to the control of nucleotide-mediated signaling during postnatal development.

Results of our study show that, although NTPDase3 mRNA is already present at PD7, NTPDase3-*ir* that resembles the enzyme localization in the adult appears in the lateral hypothalamic areas only at the end of third postnatal week (PD20), at about the time when the animals acquire the adult-like diurnal rhythms of feeding and sleeping behavior. This implies

that the developmentally regulated expression of NTPDase3 and ATP signaling may be important in the regulation of the homeostatic mechanisms involved in sleeping and feeding.

2. Materials and Methods

2.1. Animals

Female rats of Wistar strain from local colony of VINČA Institute of Nuclear Science breeding stock were used in all experiments. All procedures were carried out in accordance with the principles from Guide for Care and Use of Laboratory Animals (NIH publication no. 80-23), and the Ethical Committee for the Use of Laboratory Animals of VINČA Institute of Nuclear Sciences, University of Belgrade, Belgrade, Serbia, (02/11) approved the protocols. Animals were housed under standard conditions: 12 h light/dark regime, constant ambient temperature (22 ± 2°C) and free access to food and water.

Females were organized in the following groups: postnatal 7- (PD7), 15- (PD15), 20- (PD20), 30- (PD30) and 90- (adult) days old rats. Rats in PD7, PD15 and PD20 groups were kept in the litter, while the animals in PD30 and adults were weaned at the 21st postnatal day and kept 3/cage. At each postnatal group, rats (n= 9) were selected from at least five separate litters (reducing litter size uniformly).

Adult rats were divided into 3 groups: OVX group (n= 9/group) was subjected to bilateral ovariectomy through one dorsal incision under ketamine (50 mg/kg) and xylazine (5 mg/kg) anesthesia. The same procedure was conducted on the sham group (n= 6/group), without removal of ovaries. Intact (n= 14) animals were taken in diestrus phase of the estrous cycle were used as a control. Vaginal lavage was performed between 9-10 am during two weeks and the stage was determined by evaluating relative proportion of epithelial nucleated cells, squamous cells and leucocytes in vaginal smears. The presence of leukocytes in the smear indicated diestrus. Only those animals with regular 4-5 days cycle were included. OVX and sham animals were sacrificed 3 weeks after the surgery. Since sham operation had not

induced any significant effect on the expression of NTPDase3, those data were not discussed or included in the graphs.

2.2. Preparation of subcellular fractions

Subcellular localization of NTPDase3 and specificity of the antibodies used in the immunohistochemical study was tested by Western blot analysis, after resolving sample proteins by SDS-PAGE electrophoresis. Crude membrane fraction (P2), gliosomes, synaptosomes, purified synaptic plasma membranes, synaptic mitochondria and the cytosolic fractions were isolated from whole cerebral cortex and hippocampal formation of adult female rats by differential centrifugation on discontinuous Percoll gradient (Dunkley *et al.*, 2008; Moutsatsou *et al.*, 2001). Due to small sample size, the only fraction prepared from the dissected hypothalamic tissue was the P2 fraction.

Cortices, hippocampi and hypothalami were dissected and homogenized in 10 volumes of ice cold isolation buffer (0.32 M sucrose, 5 mM Tris-HCl, pH 7.4) in a Teflon/glass homogenizer (clearance 0.20 mm) at 900 rpm. Crude nuclear fraction and cell debris were removed by centrifugation at 1000 × g for 10 min. Supernatants were collected and centrifuged at 17000 × g for 20 min in order to obtain crude membrane fraction (P2). The P2 pellet isolated from the hypothalamus was lysed in hypo-osmotic solution (5 mMTris-HCl, pH 7.4), aliquoted and kept on –80ºC until use. P2 fractions isolated from the cortices and hippocampi were resuspended in the isolation buffer, placed on a discontinuous Percoll (Sigma-Aldrich, Munich, Germany) gradient (2, 6, 15, and 23% v/v of Percoll in 0.32 M sucrose and 1mM EDTA, pH 7.4) and centrifuged at 35000×g for 5 min. The bands containing gliosomal (Glio) and synaptosomal (Syn) fractions were removed from 2 to 6 % and 15 to 23 % Percoll interface, respectively, diluted in the isolation buffer and pelleted by centrifugation at 14000 × g for 20 min at 4 ºC to remove myelin. The synaptosomal fraction was re-suspended in 5 mMTris-HCl, pH 7.4, centrifuged at 15000 × g for 20 min at 4 ºC.

Supernatant was collected as synaptic cytosol (Cit), while the pellet was placed on a discontinuous sucrose gradient (0.32, 0.8, 1.0, and 1.2 M in 5 mM Tris-HCl, pH 7.4) and centrifuged at 90 000 × g for 2 h. Synaptic plasma membrane (SPM) fraction was collected from the 1.0/1.2 M sucrose interface, while the pellet containing synaptic mitochondria (Mit) and both fractions were resuspended in 5 mM Tris-HCl, pH 7.4, centrifuged and resuspended in sample loading buffer for immunoblotting. All steps were carried out at 4ºC.

In order to validate the effective separation of sub-cellular fractions, Western blot analysis was used to determine the abundance of well-known astrocyte (glial fibrillary acid protein) and synapse marker proteins (synaptophysin, syntaxin, PSD-95) between gliosome and synaptosome samples as well as synaptic plasma membrane, mitochondrial and cytoplasmic marker proteins (Na,K-ATPase, synaptic membrane protein; heat shock protein-60, a mitochondrial matrix protein; α-tubulin, cytoplasmic protein).

The protein content was determined using bovine serum albumin (BSA) as a standard (Markwell *et al.,* 1978).

2.3. Western blot analysis

Western blot analysis was performed as previously described (Grkovic *et al.,* 2014). Briefly, equivalent amounts (40 μg of proteins) were resolved by SDS-PAGE electrophoresis (4–8%) and transferred onto PVDF support membranes (0.45 μm, Millipore, Germany). After washing in TBST (50 mM Tris-HCl pH 7.4, 150 mM NaCl, 0.05 % Tween 20), the membranes were blocked in 5 % BSA in TBST for 1 h. The membranes were then incubated with rabbit anti-rat NTPDase3 (KLH14 antisera; a kind gift from Dr. T.L. Kirley, University of Cincinnati, OH, USA) or goat anti-β-actin antibody (Santa Cruz Biotechnology, Inc. Dallas, Texas, USA), both 1:2000 in TBST, overnight at 4°C. After washing with TBST, membranes were incubated with appropriate secondary antibodies conjugated to horseradish peroxidase (1:10000 in TBST, Santa Cruz Biotechnology, Inc. Dallas, Texas, USA).

Visualization of the bands was performed on X-ray films (AGFA HealthCare NV, Septestraat, Mortsel, Belgium) with the use of chemiluminescence (Immobilon Western Chemiluminescent HRP substrate, Millipore, Darmstadt, Germany). Densitometric analysis was performed using *ImageJ* software package while optical density of each NTPDase3 band was normalized to appropriate optical density obtained for β-actin. The results acquired from six separate measurements isolated from three animals are expressed as mean ± SEM.

2.4. Analysis of gene expression by semi-quantitative RT-PCR and qRT-PCR

The gene expression analysis of NTPDase3 was performed by a semi-quantitative RT-PCR assay as previously described (Grkovic *et al.*, 2014). The total RNA extractions from whole hypothalamus, cerebral cortex and hippocampal formation were performed using TRIzol reagent (Invitrogen, Carlsbad, CA, USA) in accordance with the manufacturer's instructions while complementary DNA (cDNA) species were synthesized using High Capacity cDNA Reverse Transcription Kit (Thermo Fisher Scientific, Waltham, MA, USA). cDNAs were amplified using primers designed for the amplification of NTPDase3 (f: 5'-CGGGATCCTTGCTGTGCGTGGCATTTCTT-3'; r: 5'-TCTAGAGGTGCTCTGGCAGGAATCAGT-3'), together with reference gene glyceraldehide-3-phosphate dehydrogenase (GAPDH, f: 5'-AAGGTGAAGGTCGGAGTCAACG-3'; r: 5'-GGCAGAGATGATGACCCTTTTGGC-3').

For polymerase chain reaction (PCR), appropriate dilutions of cDNA samples representing 2.5 μg total RNA were mixed with PCR buffer containing 10 mM deoxyribonucleoside triphosphate, 2.1 mM $MgCl_2$, 0.25 μM primers for NTPDase3, 0.125 μM primers for GAPDH and 1-U Taq polymerase (Kapa Biosystems, Wilmington, Massachusetts, USA), in a total volume of 25 μl. The cDNAs were amplified for 28 cycles (Thermal Cycler, Eppendorf), using the following conditions: denaturation 94 °C/45 s, annealing 58 °C/1 min, extension 72 °C/1 min, and final extension 72 °C/7 min. The PCR

products were analyzed on a 2 % agarose gel and visualized under UV light using ethidium bromide. Densitometry of PCR products was performed with ImageJ software package and relative NTPDase3 band intensity was normalized to GAPDH.

Quantitative real-time PCR was performed using SYBR Green (Applied Biosystems) and QuantStudio™ 3 System (Thermo Fisher Scientific, Waltham, MA, USA) using the following thermal profile parameters for both examined genes: 2 min at 50°C, 10 min at 95°C, 15 s at 95°C and 1 min at 60°C (last two steps repeated in 40 cycles). NTPDase3 gene expression levels were determined by the comparative 2^(-delta Ct) quantification method, using GAPDH as a reference gene. Samples obtained from 5 animals for each experimental group were ran in duplicate. Across the investigated groups, GAPDH gene expression remained stable, justifying its use as a reference gene. The following primers were used: NTPDase3: (f) 5'-ACGGTTACAGCACCACCTTC, (r) 5'-ACAGCTGTGGGTCACCAGTT-3'; GAPDH: (f) 5'-GTGGACCTCATGGCCTACAT-3' (r) 5'-GGATGGAATTGTGAGGGAGA-3'. The results are expressed as mean ± SEM.

2.5. Tissue processing and immunohistochemistry

Brains from examined postnatal groups (n= 3-4/group) were carefully removed from the skulls and fixed overnight in 4% paraformaldehyde in 0.1 M phosphate buffer (pH 7.4). After cryoprotection in graded sucrose, brains were frozen in 2-methyl butane and kept at –70°C until sectioning on cryotome. Sections, 25-µm thick, were mounted on gelatin-coated slides, dried for 2 h at room temperature and stored at −20 °C until use.

NTPDase3 immunolabeling was performed according to the procedure previously described (Bjelobaba *et al.*, 2010). Briefly, non-specific binding was reduced with 5% normal donkey serum in 0.01 M phosphate buffered saline pH 7.4 (PBS). NTPDase3 antiserum in 5% normal donkey serum in PBS (1:500) was applied for 1 h, at room temperature. Horseradish peroxidase conjugated secondary donkey anti-rabbit antibody (1:200; Santa Cruz

Biotechnology, Inc. Dallas, Texas, USA) was used and the reaction product was visualized with 3′3-diaminobenzidine (DAB, Dako, Glostrup, Denmark) according to manufacturer instructions. Negative control was performed by omitting the NTPDase3 antisera. Additional negative control was done using the pre-immune serum (supplied also by Dr. T.L. Kirley). In both cases, staining did not result in specific labeling. After dehydration and clearing, sections were mounted with DPX Mounting medium (Fluka, Buchs, Switzerland) and examined under Zeiss Axiovert microscope (Zeiss, Jena, Germany). Neuroanatomical regions were identified and labeled according to the rat brain atlas (Paxinos and Watson, 2005).

Double labeling procedures were performed as follows: after incubation in NTPDase3 antibody, secondary donkey anti-rabbit Alexa Fluor 555 antibody (1:200 dilution; Invitrogen, Carlsbad, CA) was applied for 2 h. The sections were washed in PBS and incubated in the primary antibodies: mouse anti-syntaxin1 (1:200 dilution; Santa Cruz Biotechnology, Inc. Dallas, Texas, USA) or mouse anti-postsynaptic density protein 95 (PSD-95; 1:200 dilution; Millipore, Billerica, MA, USA). Secondary donkey anti-mouse Alexa Fluor 488 (1:200 dilution; Invitrogen, Carlsbad, CA, USA) was applied for 2 h. Bovine serum albumin (BSA, Serva, Heidelberg, Germany) was used to block the unspecific labeling as 1% solution in PBS. All primary and secondary antibodies were diluted in 1% BSA in PBS and separately applied. Antigen retrieval step in the heated citrate buffer (pH 6) and tissue permeabilization with 0.3% Triton X-100 in PBS were performed in order to enhance the staining. The sections were mounted in mowiol (Calbiochem, Darmstadt, Germany) and examined under the Zeiss Axiovert fluorescent microscope (Zeiss, Jena, Germany) equipped with a camera and EC Plan-Apochromat 100× objective, using the Apotome system to obtain optical sections. Images were sized, cropped and their brightness and contrast were adjusted in Photoshop CS.

2.6. Data analyses

The results from PCR and Western blot analyses were presented as mean ± SEM. Significance of difference between the data obtained from intact and OVX female groups was determined using Student's *t* test. A one-way analysis of variance (ANOVA) followed by Tukey's post hoc test (considering $p<0.05$ as significant) was used to determine the significant changes in messenger RNA (mRNA) abundance between different age groups.

3. Results

3.1. Antisera specificity

The validity of the NTPDase3 antisera in the rat brain fractions was confirmed by Western blot analysis after resolving particulate subcellular fractions isolated from hypothalamus (Fig. 1A), cortex (Fig. 1B) and hippocampus (Fig. 1C) by SDS-PAGE gel electrophoresis. One major band at approximately 80 kDa was detected in the crude membrane fraction (P2), together with two faint bands at ~ 25 and 250 kDa. In accordance with the previously described localization of NTPDase3 in astrocytes and neurons (Belcher *et al*., 2006; Wink *et al*., 2006; Kiss *et al*., 2009; Bjelobaba *et al*., 2010), we found that NTPDase3 was more abundant in synaptosomal (Syn) and synaptic plasma membrane (SPM) fractions than in gliosomal (Glio) and synaptic mitochondrial (Mit) fractions, whereas the band was absent from the cytosolic fractions (Cyt). When the pre-immune serum was used, 80 kD band could not be detected, further confirming that this bend corresponds to fully glycosylated NTPDase3 membrane protein.

3.2. Syntaxin-1 and PSD-95 double immunofluorescence

Since NTPDase3 protein was detected in the Syn and SPM fractions, which both contain presynaptic and postsynaptic membrane compartments, fine synaptic localization of NTPDase3 was next determined by means of double immunofluorescence histochemistry, using the antibodies against syntaxin, as a marker of a presynaptic compartment and PSD-95, as a marker of a postsynaptic compartment. NTPDase3-immunofluorescence was only

sporadically observed in association with the fluorescence corresponding to syntaxin (Fig 1D a-c), whereas much more frequently with the fluorescence corresponding to PSD-95 (Fig. 1D d-f), indicating that NTPDase3-expressing varicosities more often represent postsynaptic elements of the synapses. However, the vast majority of NTPDase3-*ir* did not co-localize with neither of the two synaptic markers.

3.3. *NTPDase3 expression in hypothalamus, cerebral cortex and hippocampus of intact and OVX females*

To evaluate the influence of ovarian steroids on NTPDase3 gene and protein expression we used OVX and control females. As shown in Figure 1, OVX affected neither mRNA (Fig. 1E), nor the protein abundance of NTPDase3 (Fig. 1F) in adult female hypothalamus, cortex or hippocampus. Therefore, subsequent immunohistochemical study was performed in intact female rats at different postnatal ages.

3.4. *NTPDase3-mRNA expression in developing hypothalamus, cerebral cortex and hippocampus*

Developmental profile of NTPDase3 gene expression was investigated in samples obtained from the hypothalamus, cerebral cortex and hippocampus at different postnatal ages (Fig. 2). The one-way ANOVA detected a significant effect of age on NTPDase3-mRNA expression [hypothalamus: $F = 8.554$; $p < 0.001$: cerebral cortex: $F = 51.411$, $p < 0.001$; hippocampus: $F = 14.088$; $p < 0.001$]. In the hypothalamus, NTPDase3-mRNA levels were stable during postnatal development and significantly increased in the adults ($p < 0.001$, Fig 2A). In the cerebral cortex, more than twofold increase in NTPDase3-mRNA abundance between PD7 and PD15 ($p<0.01$) was evidenced, with further increase seen in adults (Fig. 2B). Although lower than in hypothalamus and cortex, the expression of NTPDase3-mRNA in the hippocampal formation was stable during development and significantly increased only in adult rats ($p < 0.001$; Fig. 2C).

3.5.Developmental pattern of NTPDase3 expression in the brain

Immunohistochemical analysis using the NTPDase3 antisera revealed restricted distribution of this enzyme in the rat brain. The distribution of NTPDase3-*ir* in the rat regions of interest through postnatal development and adults is shown in Table 1.

In coronal brain sections at PD7, faint NTPDase3-*ir* was observed in neurons in dorsal hypothalamus, while *ir* fibers were not observed. Weak NTPDase3-*ir* was observed sporadically at neuronal cell bodies in the restricted diencephalic and limbic structures, such as sub-regions of the hypothalamus and the septohippocampal nucleus (data not shown).

In PD15 sections, slightly more NTPDase3-*ir* cell bodies were detected in midline diencephalic regions (Fig. 3). Similar to what was detected at PD7, ependymal lining of the dorsal part of third ventricle (D3V) was strongly positive for NTPDase3, including the cells of choroid plexus (*chp*). Prominent *ir* was also observed in cluster of cells located in the medial habenular nucleus (MHb) and molecular layer of dentate gyrus (MoDG), while scattered *ir* cells were observed in the pyramidal layer of the hippocampus. In the hypothalamus, the highest density of NTPDase3-*ir* neuronal cell bodies were observed in the ventromedial (VMH) and dorsomedial hypothalamic nucleus (DMD), arcuate nucleus (Arch) and lateral hypothalamus (LH), whereas only faint and scattered *ir* profiles were observed in the rhomboid thalamic nucleus (Rh, Fig. 3). In cortical structures, specific *ir* profiles were not observed.

In sections obtained at PD20, stronger *ir* was observed when compared to PD15. Highly scattered thin NTPDase3-*ir* fibers were also seen mostly in the superficial layers of the cortex (Fig. 4). Strong labeling of pial surface and the choroid plexus of the third ventricle was seen. Highly *ir* cell clusters were detected in the medial habenular nucleus (MHb), ventral (DMV) and compact part (DMC) of dorsomedial hypothalamic nucleus and arcuate nucleus of the hypothalamus (Arch, Fig. 4). Rare *ir* fibers with small varicosities were

observed in the hypothalamus, along the wall of the third ventricle, in the posterior hypothalamic area (PHD) and paraventricular thalamic nucleus (PVP, Fig. 4).

In PD30 sections, similar to what was observed at previous age point, clusters of *ir* cell bodies were seen in the hypothalamic nuclei around the third ventricle, including arcuate nucleus (Arch), posterior hypothalamic nucleus (PH) and dorsal part of posterior hypothalamic area (PHD) as well as in lateral hypothalamus (LH, Fig. 5). Interestingly, *ir* cell bodies were not observed in the medial habenular region, although markedly labeled cell in the region were detected at previous age point. Strong NTPDase3-*ir* labeled *chp* of the third ventricle (Fig. 5). Starting from PD30, increasing number of progressively longer NTPDase3-*ir* fibers with prominent varicosities were observed in the cortical areas, including the secondary motor area (M2), secondary somatosensory cortex (S2) and piriform cortex (Pir) as well as in the hippocampus (Hip, Fig. 5). Immunopostive fibers with varicosities were also seen in hypothalamic, thalamic and epithalamic regions, particularly along the midline of the brain.

At the adult stage, markedly stronger *ir* was detected in all regions of the forebrain. Scattered immunoreactive profiles were observed in the cortical structures including S2 and Pir as well as in the Hip, as previously described by Belcher at al. (2006). Besides the diencephalic regions with strong *ir* localized at the cell bodies, immunopositive cell bodies were observed in the lateral hypothalamus (LH, Fig. 6). High density of long NTPDase3-*ir* varicose fibers was detected in all areas of the hypothalamus, including the perifornical part of lateral hypothalamus. Particularly long NTPDase3-positive fibers were seen in dorsal posterior hypothalamic area (PHD), paraventricular thalamic nucleus (PVP) and along midline of the diencephalon, such as intermediodorsal thalamic nucleus (IMD), central medial thalamic nucleus (CM) and ventral posteromedial thalamic nucleus (VPM), as well as in the lateral septal nucleus (LSI, Fig. 6) and nucleus of the vertical limb of the diagonal band.

4. Discussion

The aim of present study was to describe developmental pattern of NTPDase3 expression in the female rat brain. Expression and localization of NTPDase3 in the brain were analyzed by qRT-PCR and immunohistochemistry. The validity of KLH14 antisera to NTPDase3 was previously established (Belcher *et al.*, 2006) and here confirmed by Western blot analysis, after resolving crude membrane proteins by SDS-PAGE electrophoresis. The antisera marked one major *ir* band at about 80 kDa, which was absent after probing the blots with the pre-immune serum. The same approach verified that NTPDase3 had almost exclusive membrane localization, including localization in specialized postsynaptic membrane subdomain.

It was shown previously that 17β-estradiol treatment induces the protein expression of NTPDase3 in both medial and lateral hypothalamus of OVX adult females (Kiss *et al.*, 2009). Our results however, revealed that OVX in adult rats does not influence gene or protein NTPDase3 expression. Together, these results imply that the basal expression of NTPDase3 is not affected by the lack of circulating estradiol, although the protein gets promptly upregulated in its presence. We therefore hypothesize that circulating 17β-estradiol does not drive the developmental changes in NTPDase3 expression, but rather serves as its modulator. However, the increase of NTPDase3 gene expression that we observe in adult rats most probably occurs at the time of puberty. Further studies should elucidate whether there are changes in hypothalamic NTPDase3 gene and protein expression across the estrous cycle and compare it with the expression in males.

Analysis of developmental pattern of NTPDase3-mRNA expression showed that the enzyme was expressed at PD7, when NTPDase3-*ir* was observed sporadically at neuronal cell bodies in the restricted diencephalic and limbic structures, such as sub-regions of the hypothalamus and the septohippocampal nucleus, while fibers expressing NTPDase3 were not

observed. Although the expression of the NTPDase3-mRNA was stable from PD7 to PD30, significant NTPDase3-*ir* was detected after PD20. The somatic NTPDase3 labeling gradually increased until the end of the third postnatal week, particularly in the collections of cells in the lateral, ventral and dorsomedial hypothalamus. At PD20, short, marginally varicose NTPDase3 containing fibers appeared in the posterior hypothalamic area, while at PD30 the fibers became longer with prominent varicosities and extended along the midline of whole diencephalon. In the adult animals, prominent NTPDase3-*ir* appeared at neuronal cell bodies in the restricted thalamic nuclei. The strongest somatic NTPDase3-*ir* was observed in the lateral hypothalamus of adult animals, whereas the complete area was traversed with NTPDase3-*ir* varicose fibers. Specifically, clusters of neurons in the dorsomedial hypothalamic nucleus, dorsal and lateral hypothalamic areas and at the thalamus /hypothalamus junction strongly expressed NTPDase3, whereas NTPDase3-*ir* fibers were spread throughout the entire diencephalon, particularly in the paraventricular thalamic nucleus, ventromedial and dorsomedial hypothalamic nuclei, the arcuate nucleus and the perifornical part of the lateral hypothalamus. Available *in situ* hybridization data suggests that in mouse, NTPDase3 is expressed in collections of cells in the pons (Website: © 2015 Allen Institute for Brain Science. Allen Brain Atlas [Internet]. Available from: http://www.brain-map.org). The localization of NTPDase3-mRNA positive neurons supports previous suggestions that this enzyme is involved in regulation of ATP signaling in auditory neurotransmission (Vlajkovic *et al.*, 2006). Therefore, at least some of the NTPDase3-*ir* fibers that are observed in the thalamus may originate from more posterior structures.

In the cortex, NTPDase3-*ir* gradually increased over time in accordance with the trend of increase in gene expression. The labeling of cell bodies was seen only in the hypothalamus, although NTPDase3-mRNA was also present in hippocampus, while the highest NTPDase3-mRNA expression was observed in the cortex. This suggests that in these structures the

NTPDase3 protein expression is below limit of detection by immunohistochemistry, or that NTPDase3 mRNA gets actively transported from hypothalamus trough axonal projections to hippocampus and cortex.

Beginning with PD7 and during maturation, prominent NTPDase3-*ir* was observed at cells of the choroid plexus as well as strong enzyme histochemical staining of this area (our unpublished observation), also shown by others in the adults (Gampe *et al.*, 2012; Langer *et al.*, 2008). The choroid plexus is innervated by adrenergic and cholinergic neurons (Lindvall and Owman, 1981) which use ATP as co-transmitter (e.g. Burnstock, 2007). ATP can also be released from other types of cells and through P2X receptors, it may regulate the function of choroid plexus and cerebrospinal fluid composition (Xiang and Burnstock, 2005). Therefore, NTPDase3 may be an important regulator of ATP availability for P2X receptors in choroid plexus.

Overall distribution of NTPDase3 containing cells and fibers in the adult rat brain overlaps with the expression pattern of hypocretin-1/orexin-A (H/O) (Belcher *et al.*, 2006; Nambu *et al.*, 1999; Peyron *et al.*, 1998). Specifically, H/O neurons have been located in discrete regions of lateral hypothalamic areas, from which they project varicose fibers throughout the neuraxis, innervating the cortex, thalamus, hypothalamus, brainstem, and spinal cord (Bittencourt and Elias, 1998; Peyron *et al.*, 1998). Of particular interest is H/O innervation of the regions controlling behavioral states, including feeding behavior and sleep regulation (Tsujino and Sakurai, 2009) which are established gradually in the early postnatal period (Redman and Sweney, 1976). The hypothalamic pattern of NTPDase3 expression obtained in the present study was also consistent with the pattern of H/O expression in the hypothalamus during postnatal development of male rats (Stoyanova *et al.*, 2010; Yamamoto *et al.*, 2000). Similarly to what we find for NTPDase3, H/O containing cells can be observed in two-week old rats (Sawai *et al.*, 2010; Steininger *et al.*, 2004; Stoyanova *et al.*, 2010) and

their number gradually increase towards the ninth postnatal week (Sawai *et al.*, 2010). However, the density of varicose H/O fibers peaks between second and third postnatal week and then remains at constant level throughout the adulthood (Steininger *et al.*, 2004). Therefore, detectable protein expression of NTPDase3 starts at the time when the H/O projection system seem to be fully mature and coincides with the developmental shift in two important autonomic functions, feeding and sleep-wake behavior. Specifically, by the end of the third postnatal week pups establish adult-like diurnal rhythms of feeding and sleeping behavior, shifting their feeding from light to dark (Redman and Sweney, 1976) and establishing sleeping during the light period (Frank and Heller, 1997a, b). Appearance of NTPDase3 at H/O containing hypothalamic structures at that particular developmental stage, suggests that NTPDase3 might be involved in this developmental shift.

In summary, our study shows that NTPDase3 is expressed at the cells of lateral hypothalamic areas and at varicose axonal projections extending from the hypothalamus during third postnatal week, at about time when the animals acquire the adult-like diurnal rhythms of feeding and sleeping behavior. Further studies aimed to examine the modulatory role of NTPDase3 system during development may increase understanding of the role of ATP in regulation of autonomic functions.

Conflict of interest statement

The authors declare that they have no competing interests.

Author's contributions

Conceived and designed the experiments: IG, IB, NN. Performed the experiments: IG, IB, NM, IL, DD. Analyzed the data: IG, IB, NN. Contributed to critically revised the manuscript: MS, JM, AH. Wrote the paper: IG, IB, NN.

Acknowledgments

The authors are grateful to Dr. Terence L. Kirley for the generous gift of KLH14 antisera used in the study. This work was supported by Ministry of Education, Science and Technological Development, Project Nos 41014 and 173044.

REFERENCES

Abbracchio, M.P., Burnstock, G., Boeynaems, J.M., Barnard, E.A., Boyer, J.L., Kennedy, C., Knight, G.E., Fumagalli, M., Gachet, C., Jacobson, K.A., Weisman, G.A., 2006. International Union of Pharmacology LVIII: update on the P2Y G protein-coupled nucleotide receptors: from molecular mechanisms and pathophysiology to therapy. Pharmacological reviews 58, 281-341.

Belcher, S.M., Zsarnovszky, A., Crawford, P.A., Hemani, H., Spurling, L., Kirley, T.L., 2006. Immunolocalization of ecto-nucleoside triphosphate diphosphohydrolase 3 in rat brain: implications for modulation of multiple homeostatic systems including feeding and sleep-wake behaviors. Neuroscience 137, 1331-1346.

Bittencourt, J.C., Elias, C.F., 1998. Melanin-concentrating hormone and neuropeptide EI projections from the lateral hypothalamic area and zona incerta to the medial septal nucleus and spinal cord: a study using multiple neuronal tracers. Brain research 805, 1-19.

Bjelobaba, I., Lavrnja, I., Parabucki, A., Stojkov, D., Stojiljkovic, M., Pekovic, S., Nedeljkovic, N., 2010. The cortical stab injury induces beading of fibers expressing ecto-nucleoside triphosphate diphosphohydrolase 3. Neuroscience 170, 107-116.

Bjelobaba, I., Stojiljkovic, M., Pekovic, S., Dacic, S., Lavrnja, I., Stojkov, D., Rakic, L., Nedeljkovic, N., 2007. Immunohistological determination of ecto-nucleoside triphosphate diphosphohydrolase1 (NTPDase1) and 5'-nucleotidase in rat hippocampus reveals overlapping distribution. Cellular and molecular neurobiology 27, 731-743.

Braun, N., Sevigny, J., Robson, S.C., Enjyoji, K., Guckelberger, O., Hammer, K., Di Virgilio, F., Zimmermann, H., 2000. Assignment of ecto-nucleoside triphosphate diphosphohydrolase-1/cd39 expression to microglia and vasculature of the brain. The European journal of neuroscience 12, 4357-4366.

Burnstock, G., 2007. Physiology and pathophysiology of purinergic neurotransmission. Physiological reviews 87, 659-797.

Cunha, R.A., Ribeiro, J.A., 2000. ATP as a presynaptic modulator. Life sciences 68, 119-137.

Dias, R.B., Rombo, D.M., Ribeiro, J.A., Henley, J.M., Sebastiao, A.M., 2013. Adenosine: setting the stage for plasticity. Trends in neurosciences 36, 248-257.

Dunkley, P.R., Jarvie, P.E., Robinson, P.J., 2008. A rapid Percoll gradient procedure for preparation of synaptosomes. Nature protocols 3, 1718-1728.

Frank, M.G., Heller, H.C., 1997a. Development of diurnal organization of EEG slow-wave activity and slow-wave sleep in the rat. The American journal of physiology 273, R472-478.

Frank, M.G., Heller, H.C., 1997b. Development of REM and slow wave sleep in the rat. The American journal of physiology 272, R1792-1799.

Gampe, K., Hammer, K., Kittel, A., Zimmermann, H., 2012. The medial habenula contains a specific nonstellate subtype of astrocyte expressing the ectonucleotidase NTPDase2. Glia 60, 1860-1870.

Grkovic, I., Bjelobaba, I., Nedeljkovic, N., Mitrovic, N., Drakulic, D., Stanojlovic, M., Horvat, A., 2014. Developmental Increase in Ecto-5'-Nucleotidase Activity Overlaps with Appearance of Two Immunologically Distinct Enzyme Isoforms in Rat Hippocampal Synaptic Plasma Membranes. Journal of molecular neuroscience 54, 109-118.

Kiss, D.S., Zsarnovszky, A., Horvath, K., Gyorffy, A., Bartha, T., Hazai, D., Sotonyi, P., Somogyi, V., Frenyo, L.V., Diano, S., 2009. Ecto-nucleoside triphosphate diphosphohydrolase 3 in the ventral and lateral hypothalamic area of female rats:

morphological characterization and functional implications. Reproductive biology and endocrinology 7, 31.
Kukulski, F., Levesque, S.A., Lavoie, E.G., Lecka, J., Bigonnesse, F., Knowles, A.F., Robson, S.C., Kirley, T.L., Sevigny, J., 2005. Comparative hydrolysis of P2 receptor agonists by NTPDases 1, 2, 3 and 8. Purinergic signalling 1, 193-204.
Langer, D., Hammer, K., Koszalka, P., Schrader, J., Robson, S., Zimmermann, H., 2008. Distribution of ectonucleotidases in the rodent brain revisited. Cell and tissue research 334, 199-217.
Lindvall, M., Owman, C., 1981. Autonomic nerves in the mammalian choroid plexus and their influence on the formation of cerebrospinal fluid. Journal of cerebral blood flow and metabolism : official journal of the International Society of Cerebral Blood Flow and Metabolism 1, 245-266.
Markwell, M.A., Haas, S.M., Bieber, L.L., Tolbert, N.E., 1978. A modification of the Lowry procedure to simplify protein determination in membrane and lipoprotein samples. Analytical biochemistry 87, 206-210.
Moutsatsou, P., Psarra, A.M., Tsiapara, A., Paraskevakou, H., Davaris, P., Sekeris, C.E., 2001. Localization of the glucocorticoid receptor in rat brain mitochondria. Archives of biochemistry and biophysics 386, 69-78.
Nambu, T., Sakurai, T., Mizukami, K., Hosoya, Y., Yanagisawa, M., Goto, K., 1999. Distribution of orexin neurons in the adult rat brain. Brain research 827, 243-260.
Paxinos G, Watson C., 2005. The Rat Brain In Stereotaxic Coordinates, Elsevier Academic Press, 5 ed
Peyron, C., Tighe, D.K., van den Pol, A.N., de Lecea, L., Heller, H.C., Sutcliffe, J.G., Kilduff, T.S., 1998. Neurons containing hypocretin (orexin) project to multiple neuronal systems. The Journal of neuroscience 18, 9996-10015.
Redman, R.S., Sweney, L.R., 1976. Changes in diet and patterns of feeding activity of developing rats. The Journal of nutrition 106, 615-626.
Rodrigues, R.J., Almeida, T., Richardson, P.J., Oliveira, C.R., Cunha, R.A., 2005. Dual presynaptic control by ATP of glutamate release via facilitatory P2X1, P2X2/3, and P2X3 and inhibitory P2Y1, P2Y2, and/or P2Y4 receptors in the rat hippocampus. The Journal of neuroscience 25, 6286-6295.
Sawai, N., Ueta, Y., Nakazato, M., Ozawa, H., 2010. Developmental and aging change of orexin-A and -B immunoreactive neurons in the male rat hypothalamus. Neuroscience letters 468, 51-55.
Smith, T.M., Kirley, T.L., 1998. Cloning, sequencing, and expression of a human brain ecto-apyrase related to both the ecto-ATPases and CD39 ecto-apyrases1. Biochimica et biophysica acta 1386, 65-78.
Steininger, T.L., Kilduff, T.S., Behan, M., Benca, R.M., Landry, C.F., 2004. Comparison of hypocretin/orexin and melanin-concentrating hormone neurons and axonal projections in the embryonic and postnatal rat brain. Journal of chemical neuroanatomy 27, 165-181.
Stoyanova, II, Rutten, W.L., le Feber, J., 2010. Orexin-A and orexin-B during the postnatal development of the rat brain. Cellular and molecular neurobiology 30, 81-89.
Tsujino, N., Sakurai, T., 2009. Orexin/hypocretin: a neuropeptide at the interface of sleep, energy homeostasis, and reward system. Pharmacological reviews 61, 162-176.
Vlajkovic, S.M., Vinayagamoorthy, A., Thorne, P.R., Robson, S.C., Wang, C.J., Housley, G.D., 2006. Noise-induced up-regulation of NTPDase3 expression in the rat cochlea: Implications for auditory transmission and cochlear protection. Brain research 1104, 55-63.

Vongtau, H.O., Lavoie, E.G., Sevigny, J., Molliver, D.C., 2011. Distribution of ecto-nucleotidases in mouse sensory circuits suggests roles for nucleoside triphosphate diphosphohydrolase-3 in nociception and mechanoreception. Neuroscience 193, 387-398.

Wang, T.F., Guidotti, G., 1998. Widespread expression of ecto-apyrase (CD39) in the central nervous system. Brain research 790, 318-322.

Website: © 2015 Allen Institute for Brain Science. Allen Brain Atlas [Internet]. Available from: http://www.brain-map.org).

Wieraszko, A., 1996. Extracellular ATP as a neurotransmitter: its role in synaptic plasticity in the hippocampus. Acta neurobiologiae experimentalis 56, 637-648.

Wink, M.R., Braganhol, E., Tamajusuku, A.S., Lenz, G., Zerbini, L.F., Libermann, T.A., Sevigny, J., Battastini, A.M., Robson, S.C., 2006. Nucleoside triphosphate diphosphohydrolase-2 (NTPDase2/CD39L1) is the dominant ectonucleotidase expressed by rat astrocytes. Neuroscience 138, 421-432.

Xiang, Z., Burnstock, G., 2005. Expression of P2X receptors in rat choroid plexus. Neuroreport 16, 903-907.

Yamamoto, Y., Ueta, Y., Hara, Y., Serino, R., Nomura, M., Shibuya, I., Shirahata, A., Yamashita, H., 2000. Postnatal development of orexin/hypocretin in rats. Brain research. Molecular brain research 78, 108-119.

Zimmermann, H., 2006. Nucleotide signaling in nervous system development. Pflugers Archiv 452, 573-588.

Zimmermann, H., Zebisch, M., Strater, N., 2012. Cellular function and molecular structure of ecto-nucleotidases. Purinergic signalling 8, 437-502.

Legends to Figures

Figure 1. A-C. Specificity of polyclonal NTPDase3 antisera. The subcellular fractions were obtained from hypothalamus (A), cortex (B) and hippocampus (C). One major NTPDase3 band at ~ 80 kDa was detected in the P2, Syn and SPM and faint band in Glio and Mit fractions, together with two faint bands at ~ 25 and 250 kDa. When the pre-immune serum was applied, 80 kDa-band could not be detected. **D**. Double immunofluorescent staining of NTPDase3 and synaptic markers. (a-c) Representative set of high magnification optical sections of cortex showing NTPDase3 (red fluorescence, a, d) and syntaxin or PSD-95 (green fluorescence, b, e) expression. Overlaid images (c, f) reveal sporadic expression of NTPDase3 in the presynaptic compartment and more frequent expression of NTPDase3 on postsynaptic elements of the synapses. Scale bar applies to all images: 10 μm. **E-F.** Expression of NTPDase3 assessed at mRNA (E) and protein (F) level in the hypothalamus, cortex and hippocampus of control (C, white bars) or OVX (gray bars) female rats. Bars represent mean ± SEM. No significant changes in NTPDase3 mRNA and protein content could be detected in any investigated region.

Figure 2. NTPDase3 gene expression in the hypothalamus (A), cerebral cortex (B), and hippocampus (C) at different ages, relative to GAPDH. Bars represent mean ± SEM. Letters a b c and d indicate significance level of $p<0.05$ or less compared with PD7, PD15, PD20 and PD30, respectively.

Figure 3. NTPDase3 staining in the coronal brain section obtained from PD15 animals. Ependymal lining of the dorsal part of third ventricle (D3V) and choroid plexus (*chp*) exhibit strong NTPDase3–*ir*. Cluster of NTPDase3-*ir* cells in the medial habenular nucleus (MHb) and molecular layer of dentate gyrus (MoDG). Faint *ir* profiles were observed in the rhomboid thalamic nucleus (Rh). Strongly labeled NTPDase3 cell bodies observed in

the dorsomedial (DMD) and ventromedial hypothalamic nucleus (VMH), lateral hypothalamus (LH), arcuate nucleus (Arch). Scale bar: 20 µm.

Figure 4. NTPDase3 staining in the coronal brain section obtained from PD20 animals. Scattered *ir* profiles were observed in superficial layers of secondary motor area (M2) and secondary somatosensory cortex (S2). Strong *ir* labels pial surface and the choroid plexus of the third ventricle (*chp*). NTPDase3-ir cells in the medial habenular nucleus (MHb) and at cells lining the third ventricle. Highly *ir* cells clusters in the ventral (DMV) and compact part (DMC) of dorsomedial hypothalamic nucleus, arcuate nucleus (Arch) and *ir* fibers with small varicosities (*arrows*) in the posterior hypothalamic area (PHD). Scale bar: 50 µm; S2 = 10 µm

Figure 5. NTPDase3 staining in the coronal brain section obtained from PD30 animals. Immunopositive fibers with prominent varicosities were observed in secondary motor area (M2), secondary somatosensory cortex (S2), piriform cortex (Pir) as well as in the hippocampus (Hip). Long NTPDase3-*ir* fibers with prominent varicosities (*arrows*) were observed in the thalamic and hypothalamic regions. Strong NTPDase3-*ir* labels choroid plexus (*chp*) of the third ventricle (D3V). Highly *ir* cell clusters in the dorsal part of posterior hypothalamic area (PHD), posterior hypothalamic nucleus (PH), lateral hypothalamus (LH) and arcuate nucleus (Arch). Scale bar: 50 µm; Hip, LH = 10 µm.

Figure 6. NTPDase3 staining in the coronal brain section obtained from adult animals. Long NTPDase3-*ir* varicose fibers were seen in posterior hypothalamic area (PHD), paraventricular thalamic nucleus (PVP) and along midline of the diencephalon: in intermmediodorsal thalamic nucleus (IMD), central medial thalamic nucleus (CM), lateral septal nucleus (LSI). Prominent NTPDase3-*ir* cells could be observed in the lateral hypothalamus (LH). Scale bar: 20 µm.

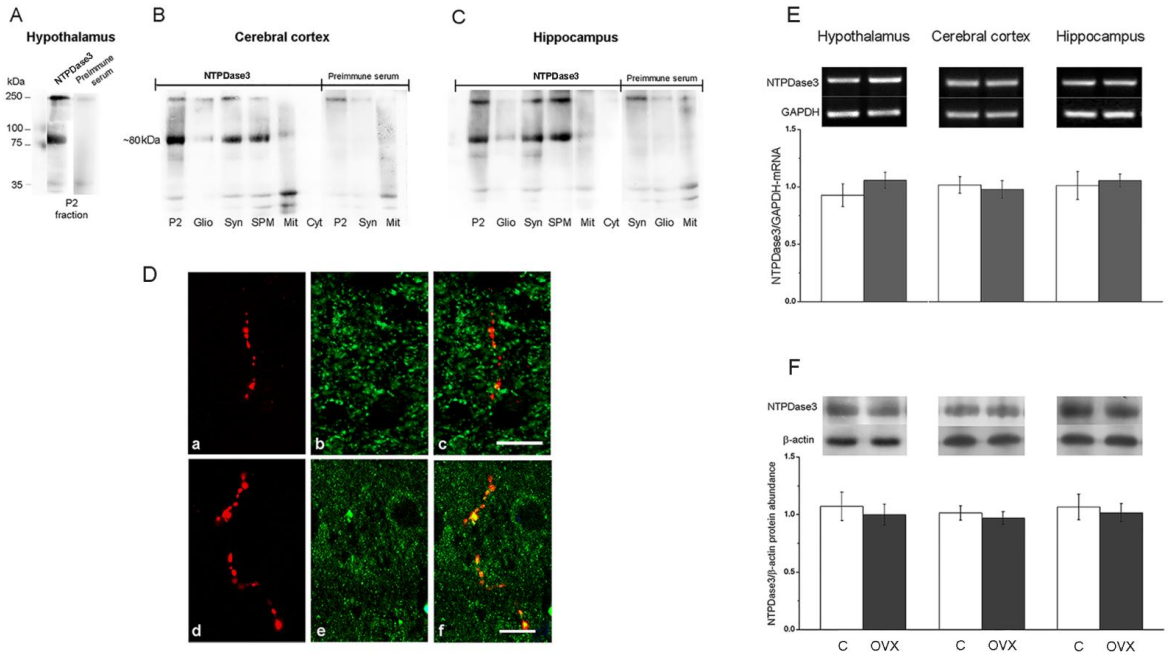

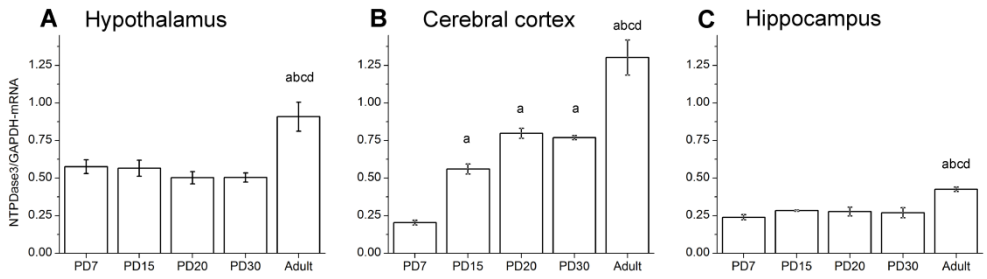

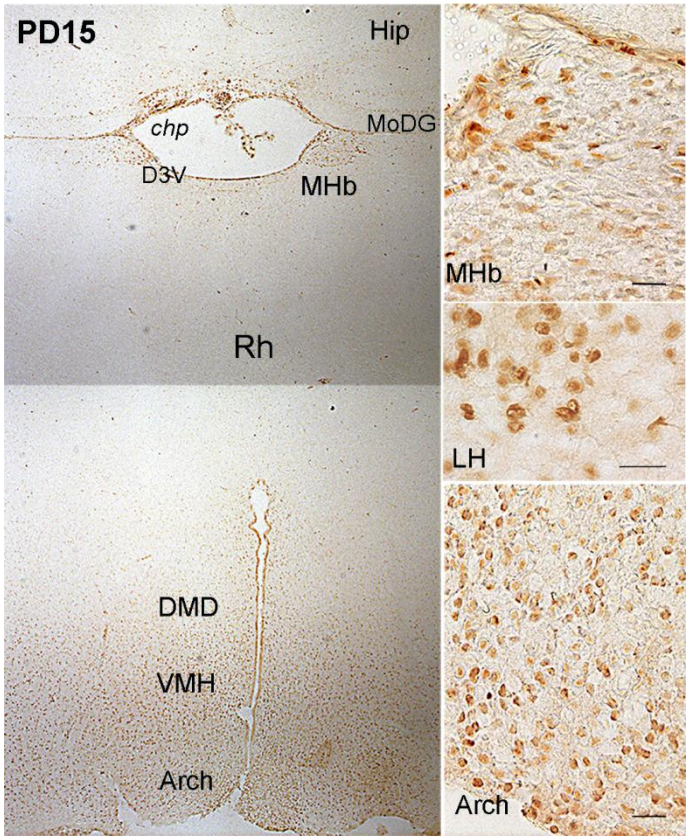

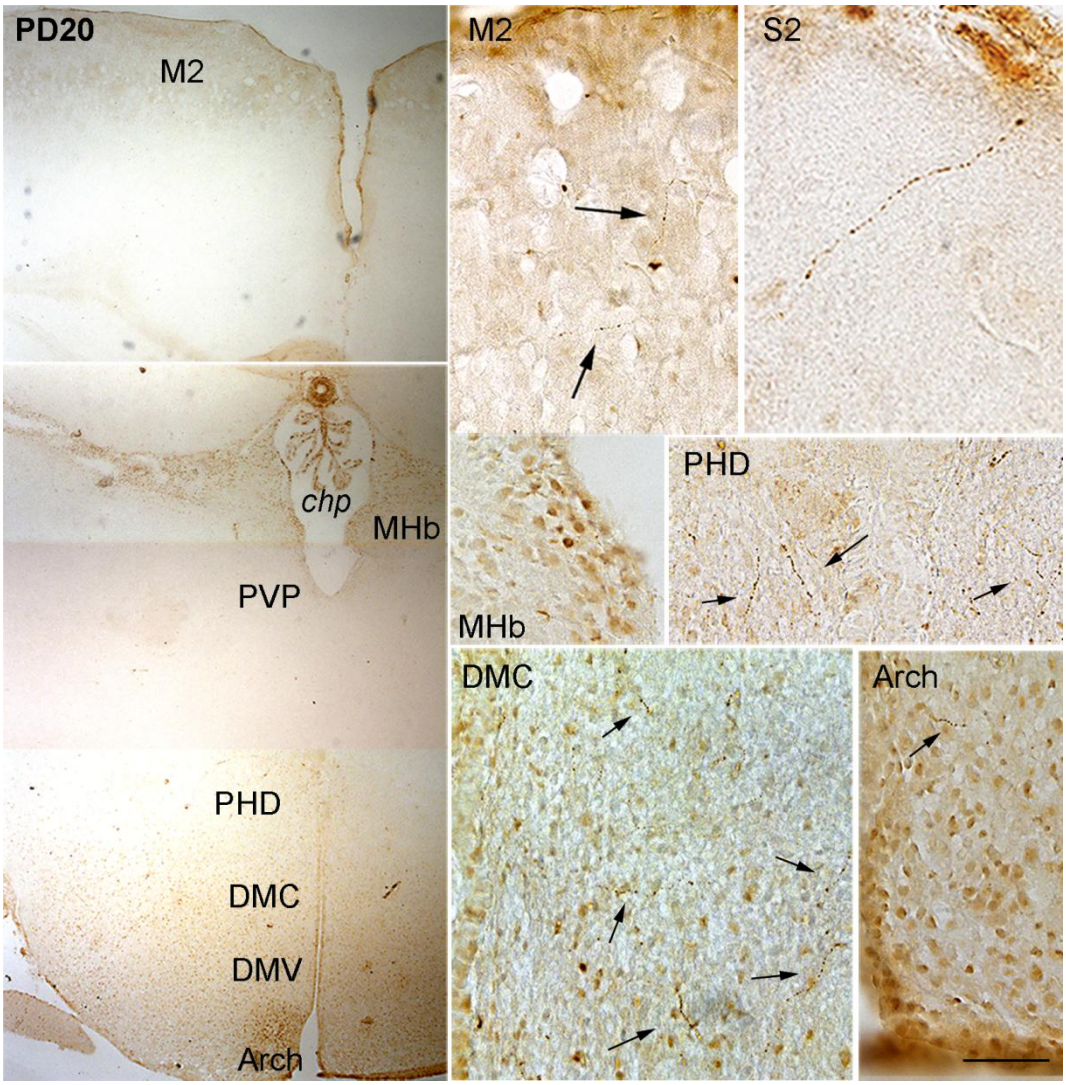

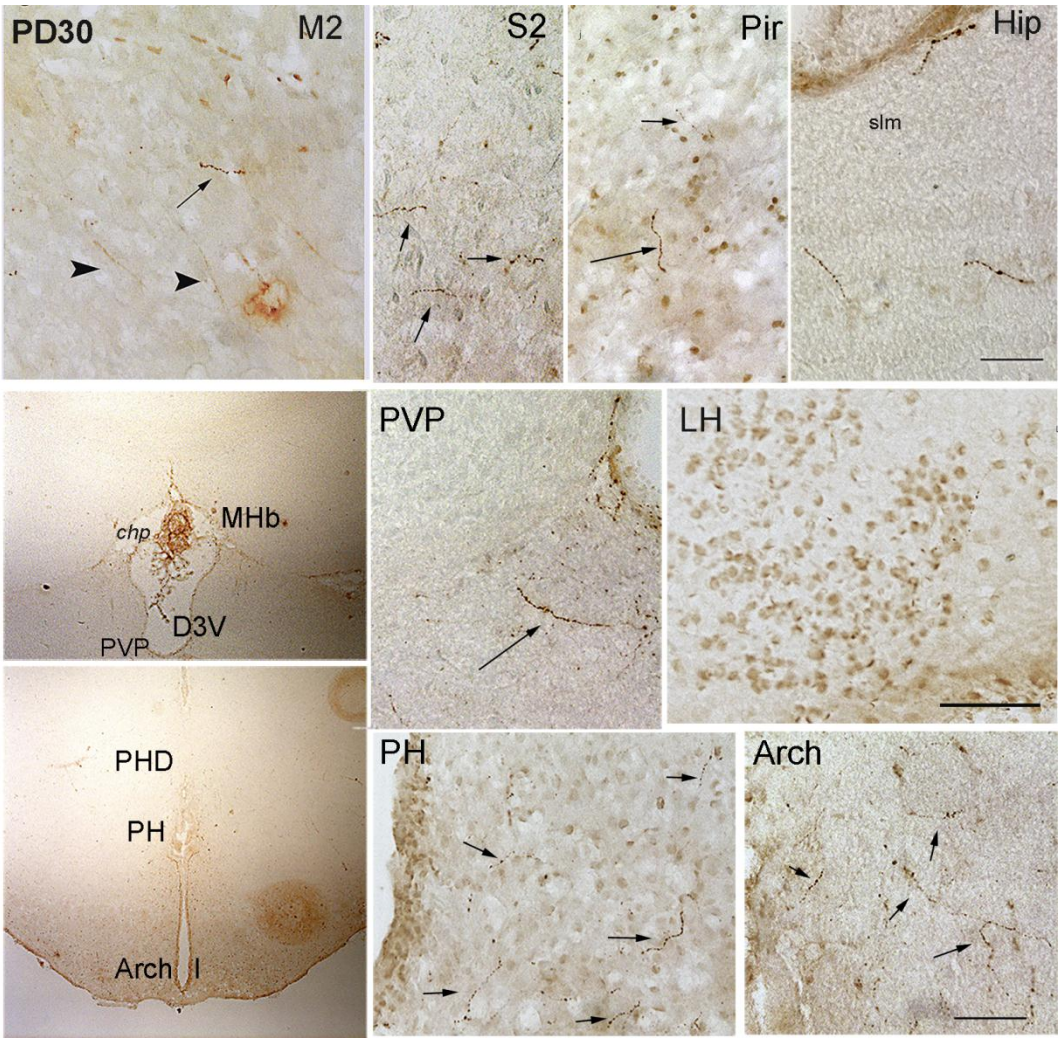

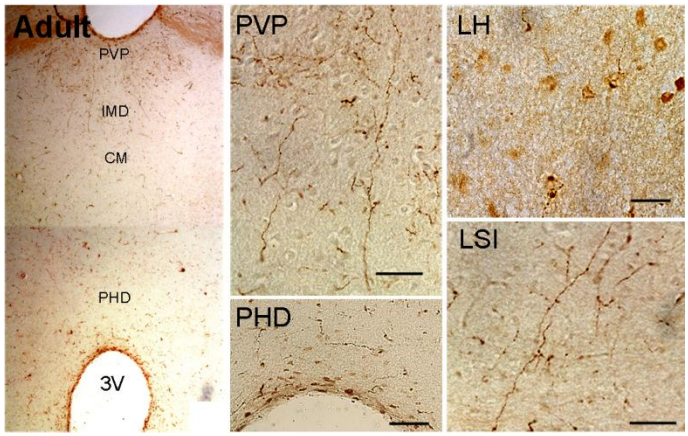

Table 1. Distribution of NTPDase3-*ir* in the rat brain at different postnatal ages

	cell bodies					varicose fibers				
Brain region	PD7	PD15	PD20	PD30	Adult	PD7	PD15	PD20	PD30	Adult
Cerebral cortex	-	-	-	-	-	-	+	+	++	++
Piriform cortex	-	-	-	-	-	-	-	-	++	++
Hippocampal formation										
Dentate girus	-	+	-	-	-	-	-	+	+	++
Hippocampus	-	+	-	-	-	-	-	+	++	++
Septohippocampal nucleus	-	-	-	-	-	-	-	+	++	++
Choroid plexus	+	++	+++	+++	++	-	-	-	-	-
D3V	++	++	+++	-	-	-	-	+	+	+
Medial habenular nucleus	-	++	+++	-	-	-	-	-	++	+++
Paraventricular thalamic nucleus			+	-	-	-	-	+	++	+++
Hypothalamus										
Medial zone	+	+++	+++	++	+	-	-	++	++	+++
Arcuate nucleus	-	++	++	++	++	-	+	+	++	++
Lateral hypothalamic area	-	++	+++	+++	++	-	-	+	++	+++
Posterior hypothalamic nucleus	-	-	-	-	-	-	+	++	++	++

Symbols designate no detectable (-), faint (+), moderate (++), and high (+++) levels of immunoreactivity